LIBS, LA-ICP-MS

Interakce laserového záření se vzorkem

Tomáš Černohorský

Univerzita Pardubice

Základní schéma LIBS

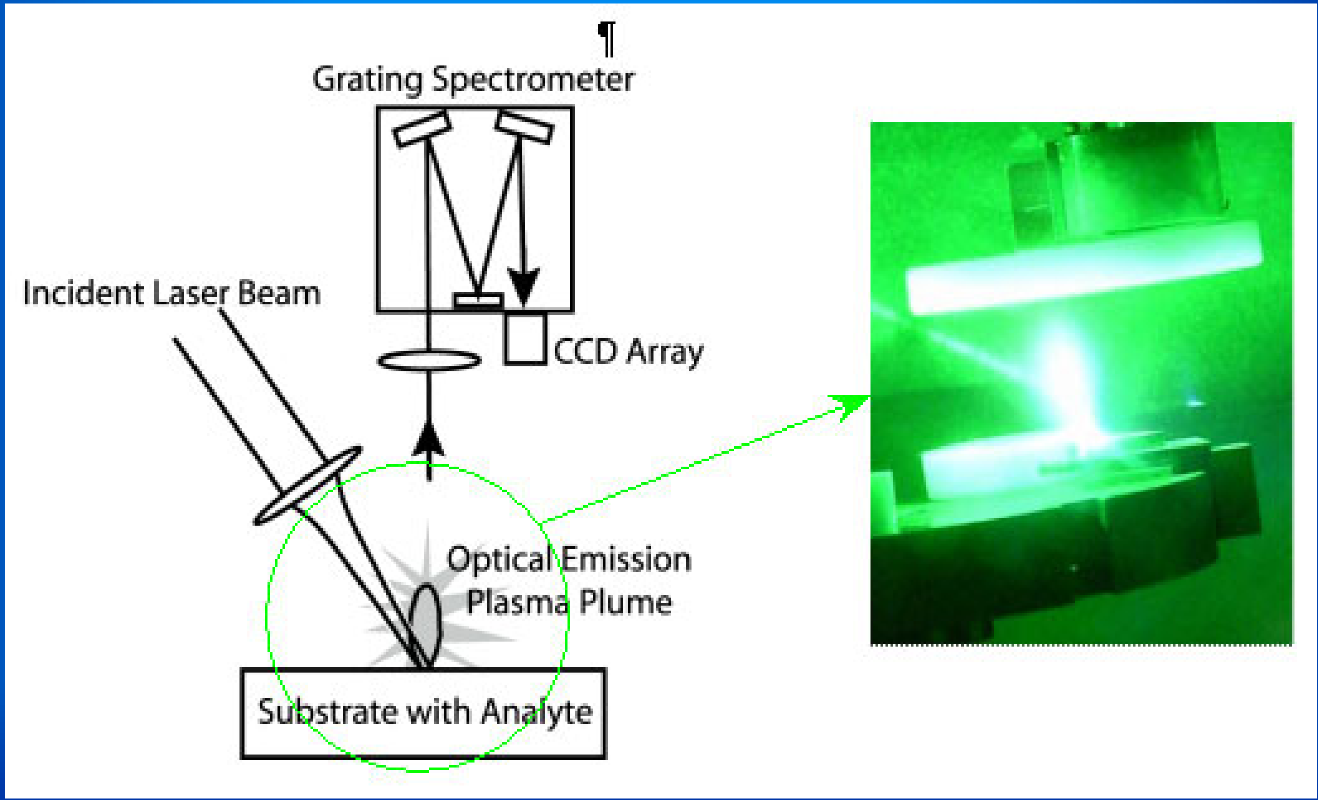

Plasma

- ionizovaný plyn
- dostatečná koncentrace nabitých částic
- navenek neutrální
- typické LIBS plasma – nižší stupeň ionizace – cca. 10%

Charakterizace plasmatu

- dána elektronovou hustotou a teplotou
- elektronová hustota – možné určit z rozšíření a hyperjemných posunů čáry – Starkův efekt
- teplota plazmatu a termodynamická rovnováha
- LTE – Local Thermodynamic Equilibrium

  - s využitím Boltzmanova rozložení

  - s využitím Sahovy rovnice

Charakterizace plasmatu

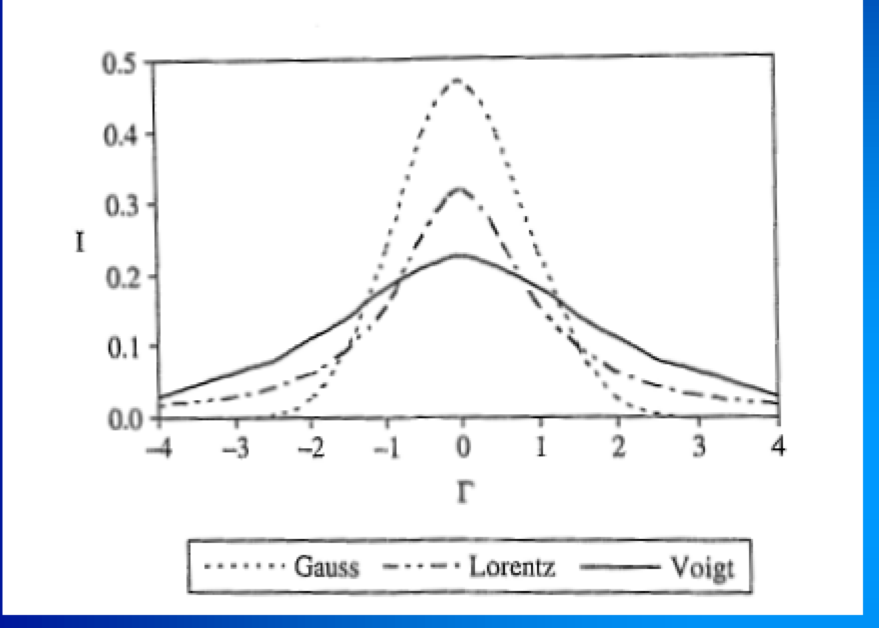

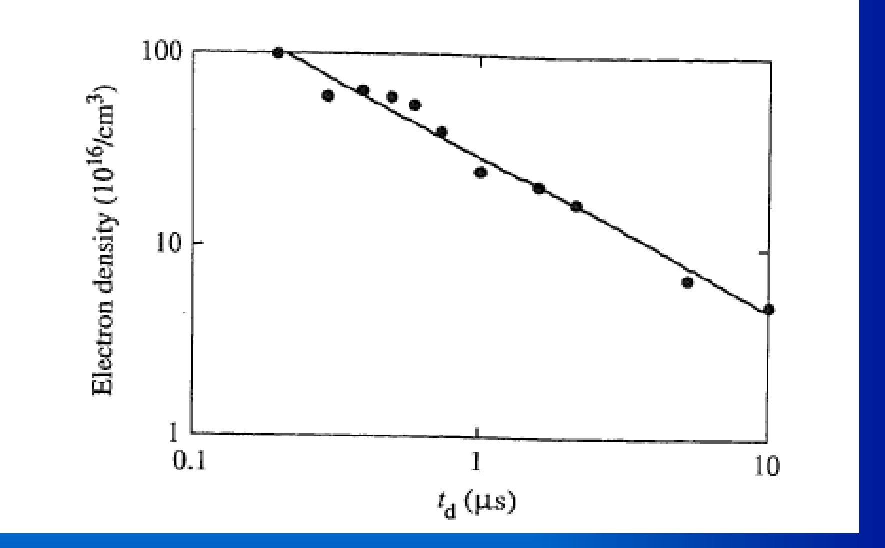

Figure 2.4 Electron densities measured in some LIBS experiments. Data abstracted from Stark widths of F, Ar, N and Cl lines

Charakterizace plasmatu

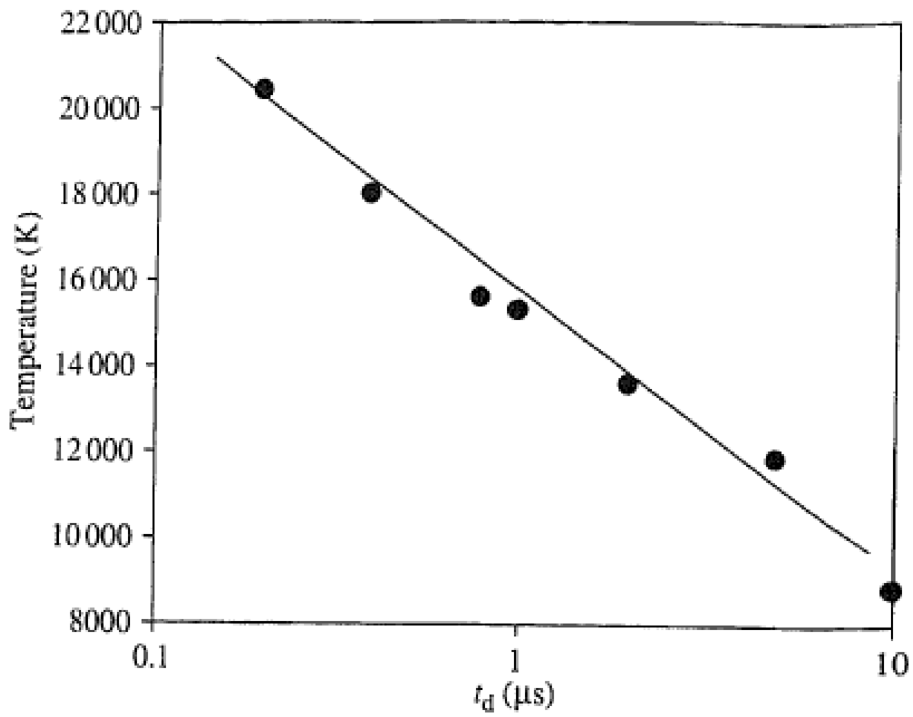

Figure 2.10 Air plasma temperature as a function of time after plasma formation using Saha and Boltzmann data from C and Be lines

Vznik LIBS plazmatu

- **Two mechanisms are responsible for growth in laser-induced breakdown**

- **Multiphoton absorption** (first step, active in focal volume)

- **Collision-induced ionization** (second step, major process in the growth)

Multiphoton absorption

- **O_2 (12.2 eV), N_2 (15.6 eV)**
- **Nd:YAG 1024 nm (1.25 eV) 532 nm (2.33 eV)**
- first step, active in focal volume
- electron density growth linear

$$\mathrm{M} + mh\nu \longrightarrow \mathrm{M}^{+} + \mathrm{e}^{-},$$

-

Collision-induced ionization

- second step, major process in the growth of plasma
- collision ionization
- electron density growth exponentially
- ionization of gas and breakdown

$$e^- + M \longrightarrow 2e^- + M^+.$$

•three body ionization (photon – electron – ion)

Breakdown Treshold

Table 1 Breakdown thresholds for various media

Test medium	Laser type	
	Ruby (0.69 μm) (10^{10} W cm^{-2})	Nd^{+3} (1.06 μm) (10^{10} W cm^{-2})
Gas[a]		
Air	20	7
Ar	8	2
He	15	4
N_2	21	9
Liquid		
Tap water[b]	3.8	10
Distilled water[c]		62
Benzene[c]		4.4
Solid[d]		
NaCl	15	14
KBr	5.7	5

[a] Pressure = 1 atm; ruby, T_p = 40 ns; Nd^{3+}, T_p = 40 ns.(8)
[b] Ruby, T_p = 21 ns, Nd^{3+}, T_p = 50 ns.(9)
[c] Nd^{3+}, T_p = 50 ns.(10)
[d] Ruby, T_p = 10 ns; Nd^{3+}, T_p = 10 ns.(11)
T_p is the laser pulse width.

Breakdown Treshold

Table 2.4 Recent measured breakdown thresholds for some laser pulses on solids

Laser, wavelength, pulse length	Surface, gas and pressure	Breakdown threshold irradiance (W/cm^2)	Reference
Nd:YAG, 532 nm, 6 ns	Cu, atm air	1.67×10^9	Semerok *et al.*, 2002
Ti:sapphire, 800 nm, 5 ps	Cu, atm air	9×10^{10}	Hashida *et al.*, 2002
Ti:sapphire, 800 nm, 70 fs	Cu, atm air	2.5×10^{11}	Hashida *et al.*, 2002
Colliding-pulse laser, 620 nm, 90 fs	$BaTiO_3$, vacuum	5×10^{11}	Millon *et al.*, 2003
Colliding-pulse laser, 620 nm, 120 fs	Fused silica, atm air	1×10^{13}	von der Linde and Schüler, 1996 (also investigated were glass, sapphire and magnesium fluoride)
Nd:YAG, 1064 nm, 6.4 ns	Fused silica, argon	5.5×10^{10}	Galt *et al.*, 2003

Time and spatial resolution of LIP

1. **Initial plasma (0 – 100 ns)**

High electron and ion densities, 20 000K

Very high continuum background emission

(bremsstrahlung)

2. **Intermediate plasma (300 ns)**

- Emission lines can be found, still high background, lines are broaden (Stark effect)

3. **Analytical plasma** – after 1 - 10 us

- Narrow lines, low background

Time and spatial resolution of LIP

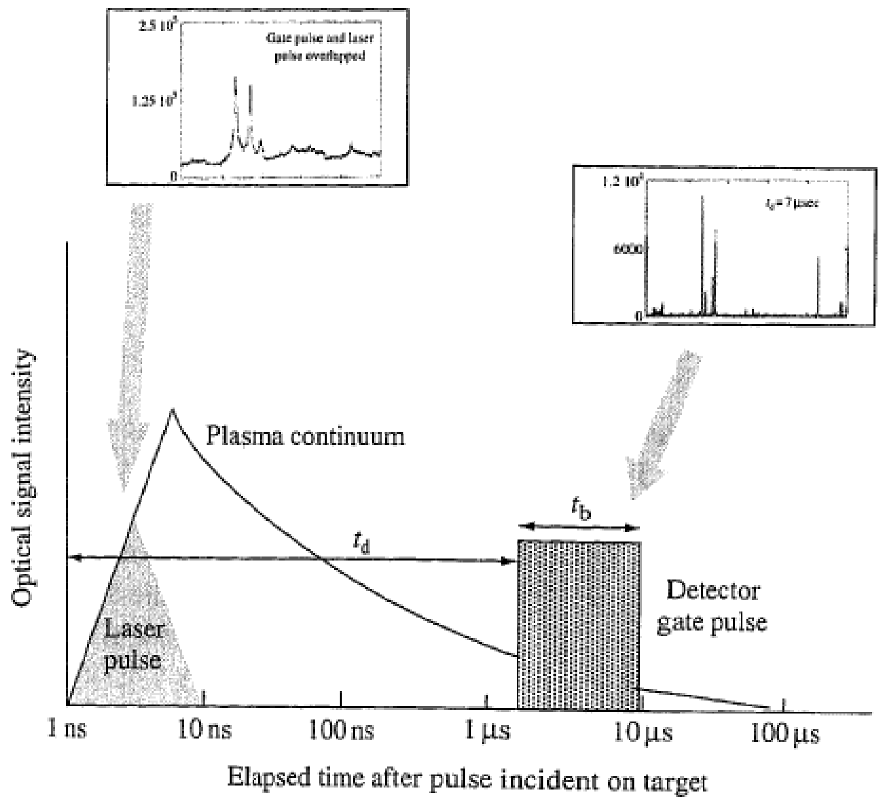

Figure 2.1 A schematic overview of the temporal history of a LIBS plasma. The delay and window are shown. Inserts illustrate the kind of spectra one might observe at the different times

Nd:YAG 1024 nm, 5 – 10 ns

Time and spatial resolution of LIP

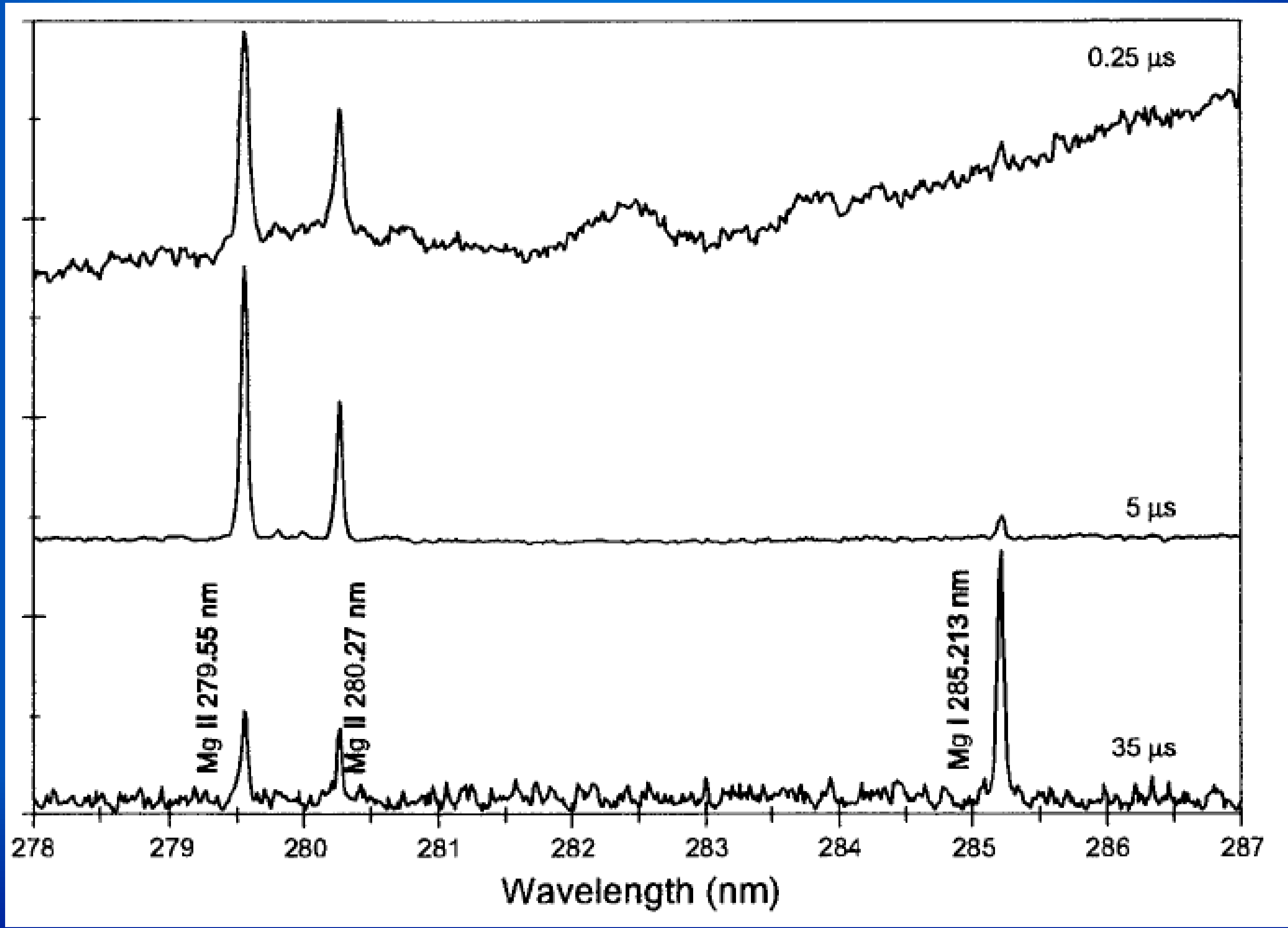

Time and spatial resolution of LIP

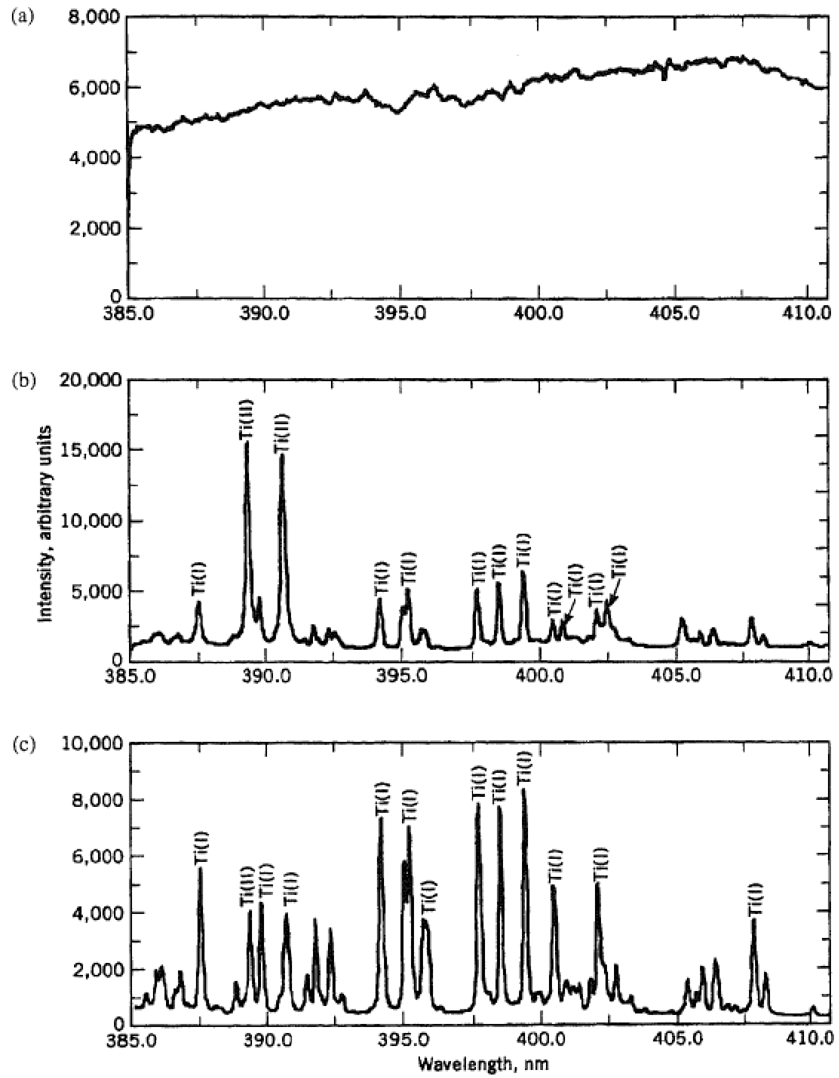

Figure 1.4 Gated titanium spectra of a LIBS plasma illustrating the development of the spectra as a function of the time after plasma initiation. The time intervals are: (a) 0–0.5 µs; (b) 0.5–5 µs; and (c) 10–110 µs

Detection Time Window

- delay between start of integration and start of laser (start of laser lamp flash) in μs
- integration window in μs (ns very expensive)

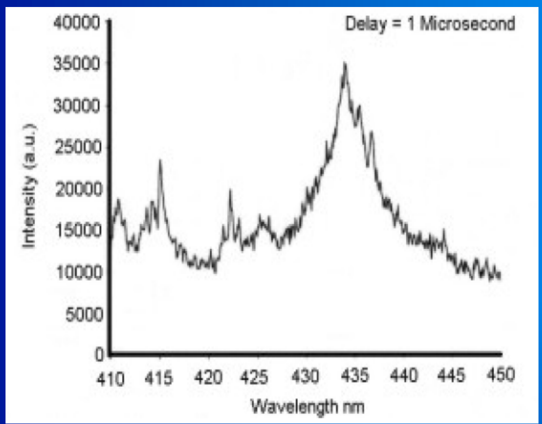

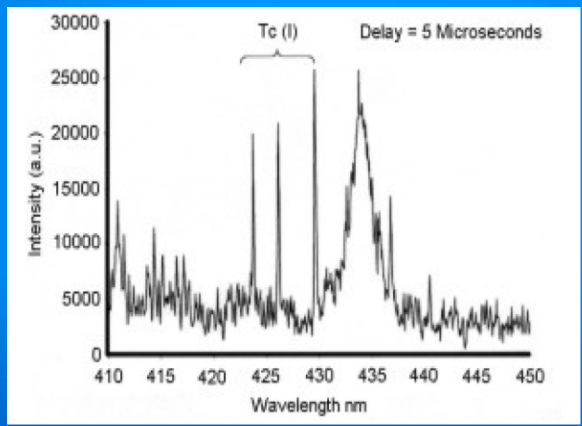

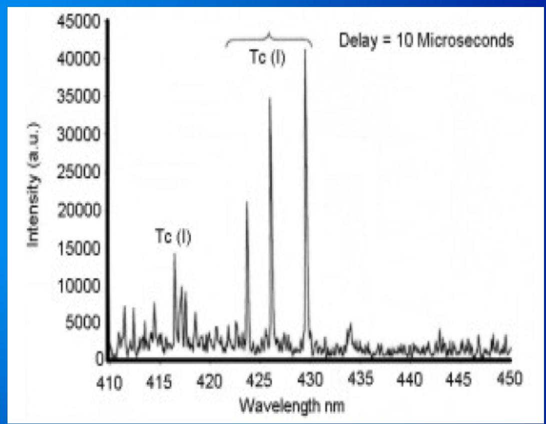

Theoretical principles of LIBS – another view

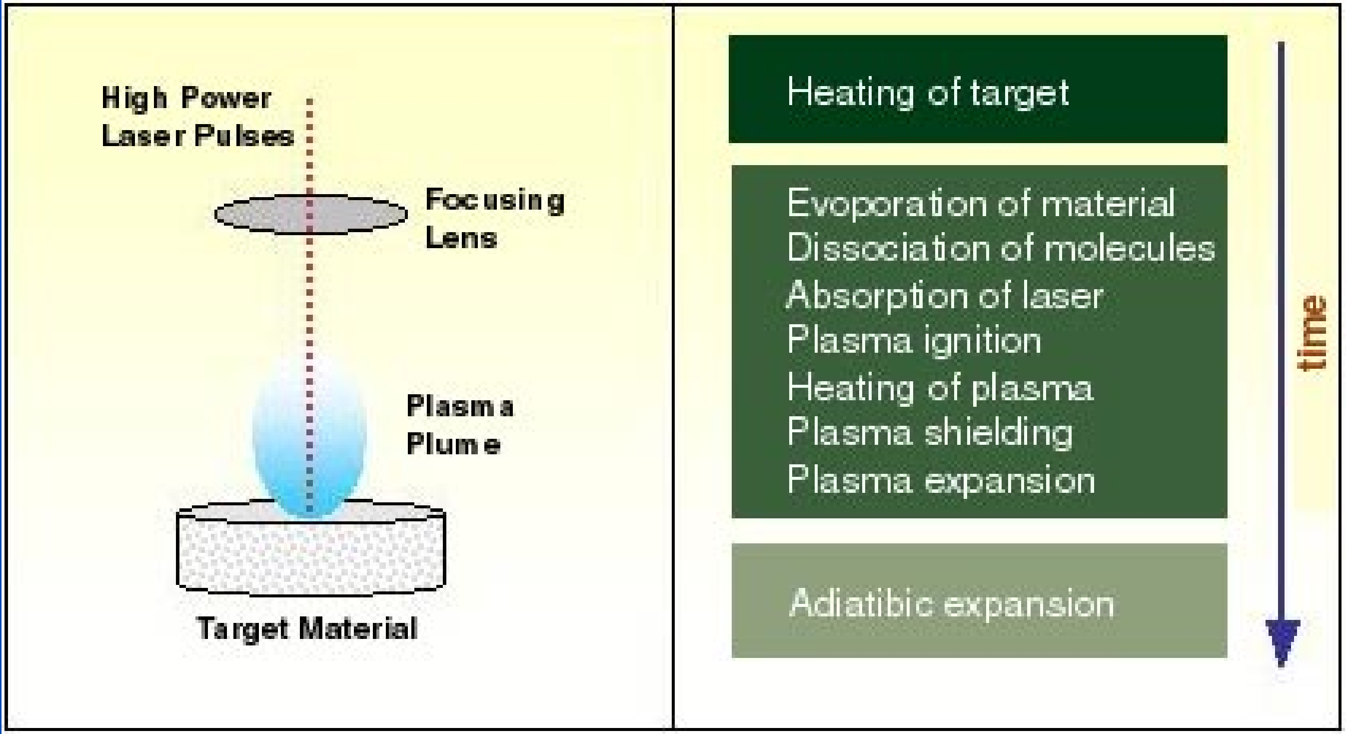

Evolution of laser induced plasma from a target material

Theoretical principles of LIBS

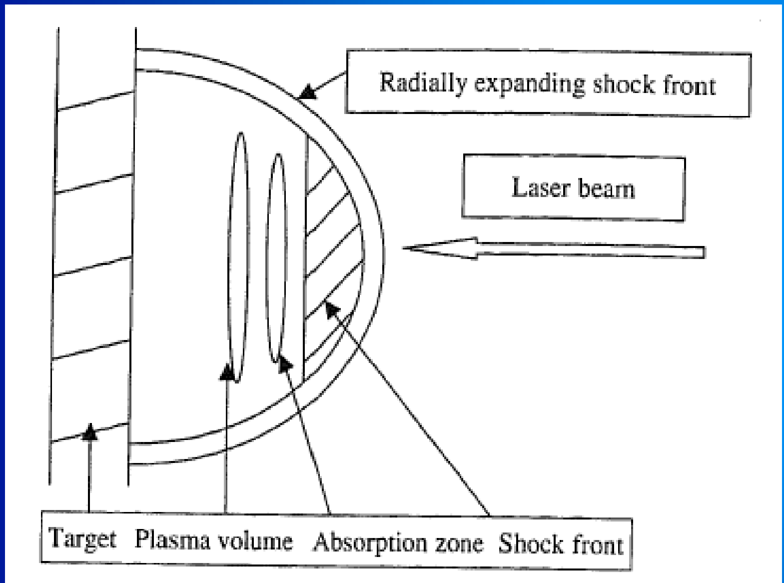

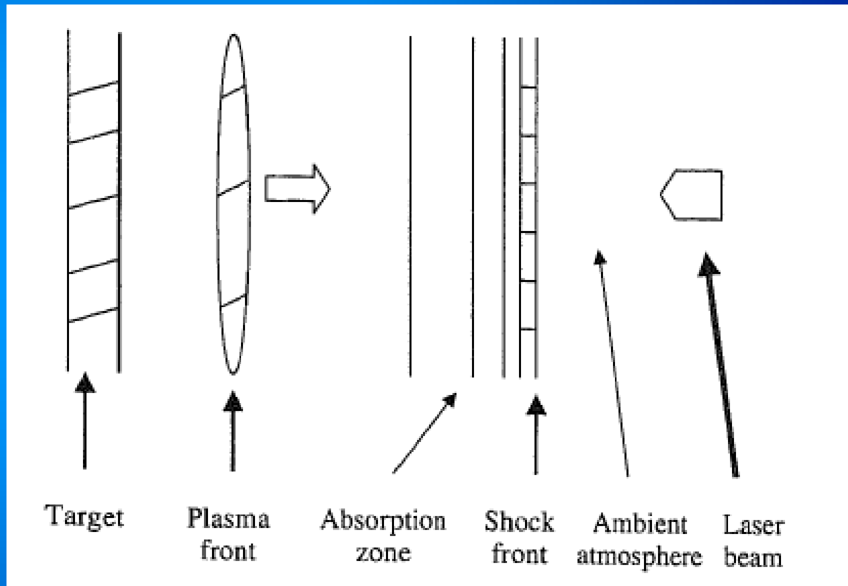

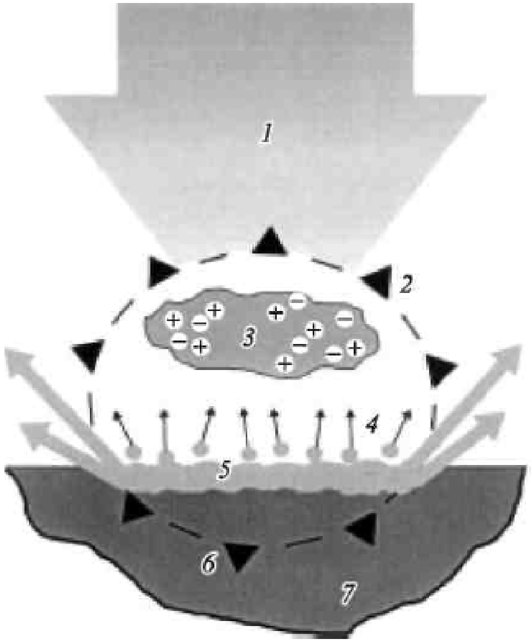

Fig.3. Diagram of laser pulse-induced physical processes in non-transparent material: 1 – laser beam; 2 – front of shock wave spreading from plasma area; 3 - plasma; 4 – material evaporation; 5 – melted material spreading out of the laser spot under the action of shock wave; 6 – front of pressure wave in material; 7 – non-transparent material.

LIBS – spatial resolution

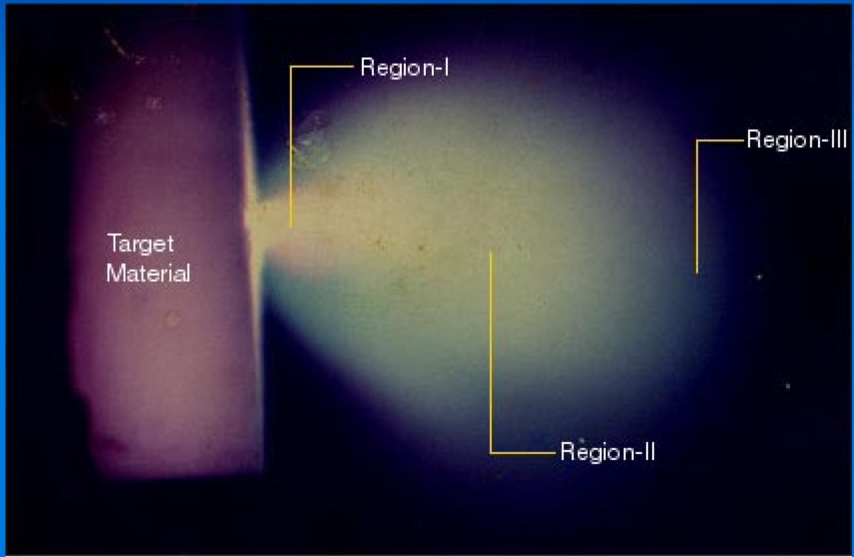

Laser produced plasma plume from a metal target

- Region-I: This is the central or core region. This is the plasma emission close to the sample surface, where the temperature is maximum and most species are in inonised state.
- Region-II: This is the mid region. Here apart from ionised species, both neutral and certain number of molecular species are present.
- Region-III: It is the extended region of the plasma. Here plasma temperature is comparatively lower and larger density of molecular species present.

Variables which effects LIBS

- Laser properties (wavelength, energy, pulse duration, shot to shot power fluctuation)
- Focusing spot size
- Ambient conditions
- Physical properties of sample
- Detection time (delay time and gate width)

Laser Parameters

- **energy – 10^9 W.cm^{-1}** and more (from 30 to 300 mJ)

- **collision-induced ionization** – dominant for long – wavelength lasers Nd:YAG **1024 nm is preferred for LIBS**

- **UV lasers**

- better energy coupling for reflective and some transparent samples

– multiphoton absorption in focal volume – responsible for aerosol production, **better for Laser Ablation**

Laser Parameters

- pulse duration – ns is best for LIBS, ps 1000x higher breakdown threshold
- geometry of laser beam – flat field
- pulse energy reproducibility

Focal Properties

• small spot – hottest plasma, lover matrix effect, problem with homogeneity

• larger spot – soft ablation, higher matrix effect

Minimal erosion spot size – dependent on the wavelength. For Nd:YAG 1024 nm – app. 30 μm, dependent on the sample type

Optimal solution:

- wide range of laser energy

- wide range of laser spot (from 2 mm to μm)

Physical properties of sample

- reflectivity
- density
- thermal conductivity
- boiling point

- High laser energy is preferable – no problems with coupling energy on reflective surfaces and with thermal conductivity. Lower segregation effect. Up to 150 mJ, higher energies – self absorption effect.

Ambient Conditions

- air – optimal for lot of elements
- Ar, lower intensity, two time higher background for high energy pulses, optimal for low energy lasers
- He – better sensitivity for most elements
- vacuum – lower intensity, plasma expand rapidly and becomes thin, better for some elements – vacuum lines C, S, P – sometimes problems with adjusting of entrance optics.

Double pulse technology

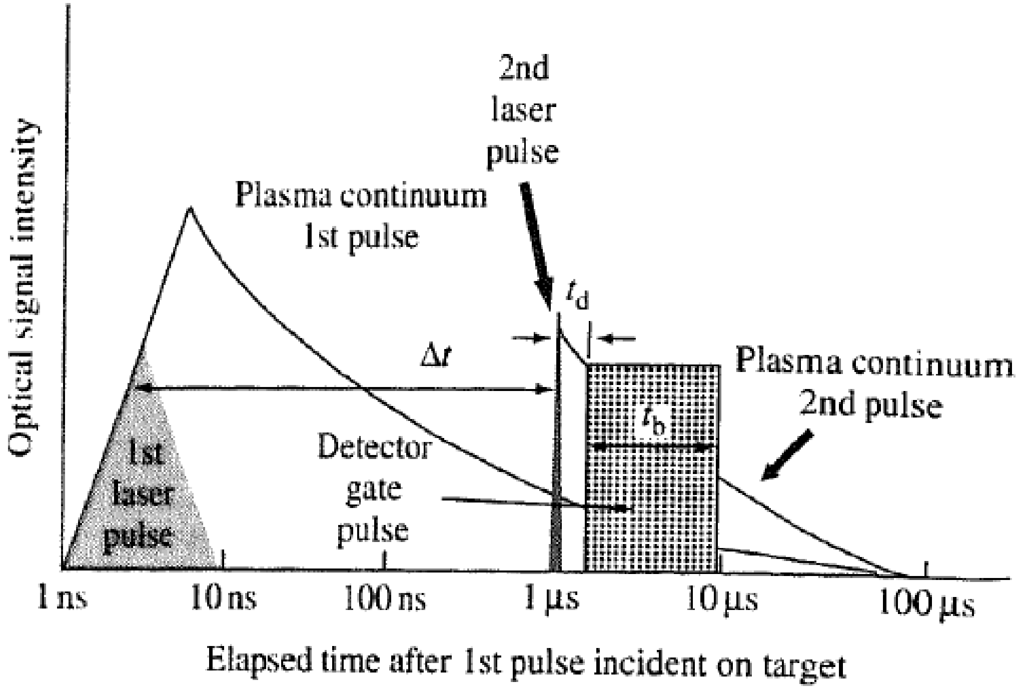

Figure 2.16 The temporal history of a LIBS plasma when two laser pulses are used. The delay between the pulses is Δt, the delay to the opening of the window t_d, and window length is t_b

Laser – Nd:YAG double pulse laser

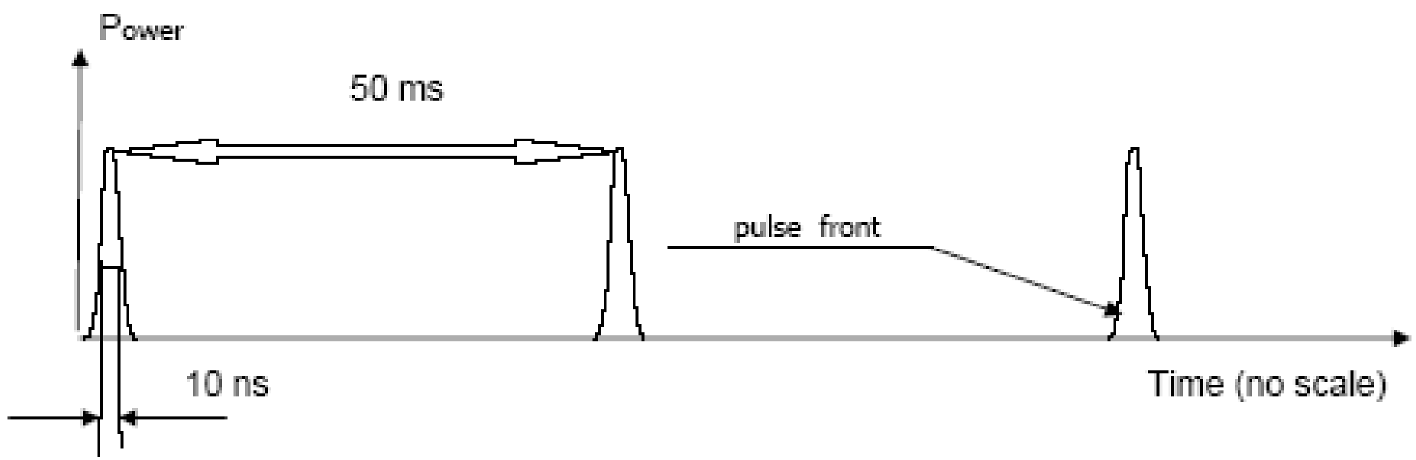

Fig.2a. Single-pulse mode of laser operation

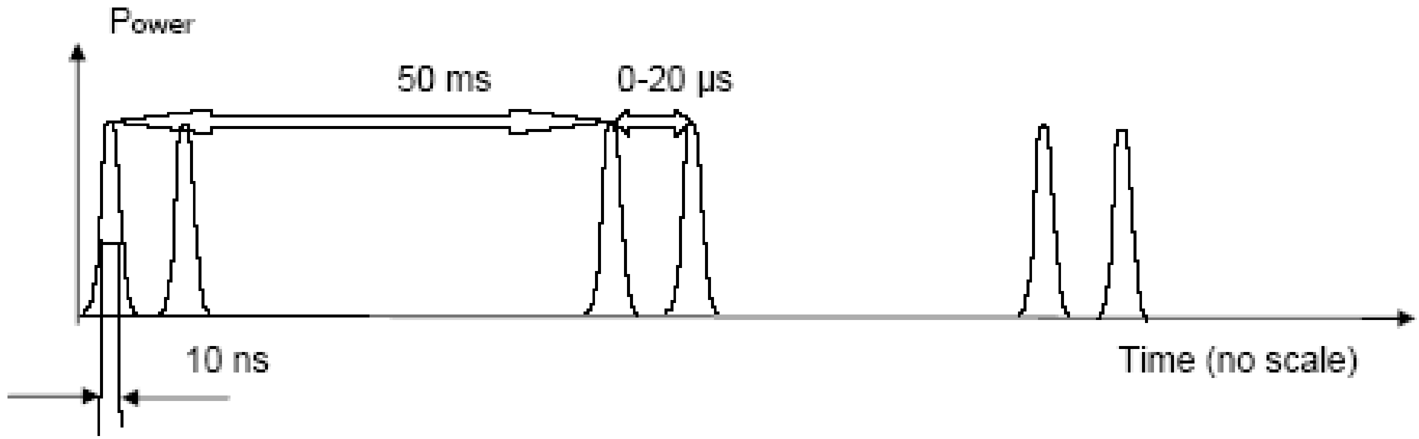

Double pulse technology

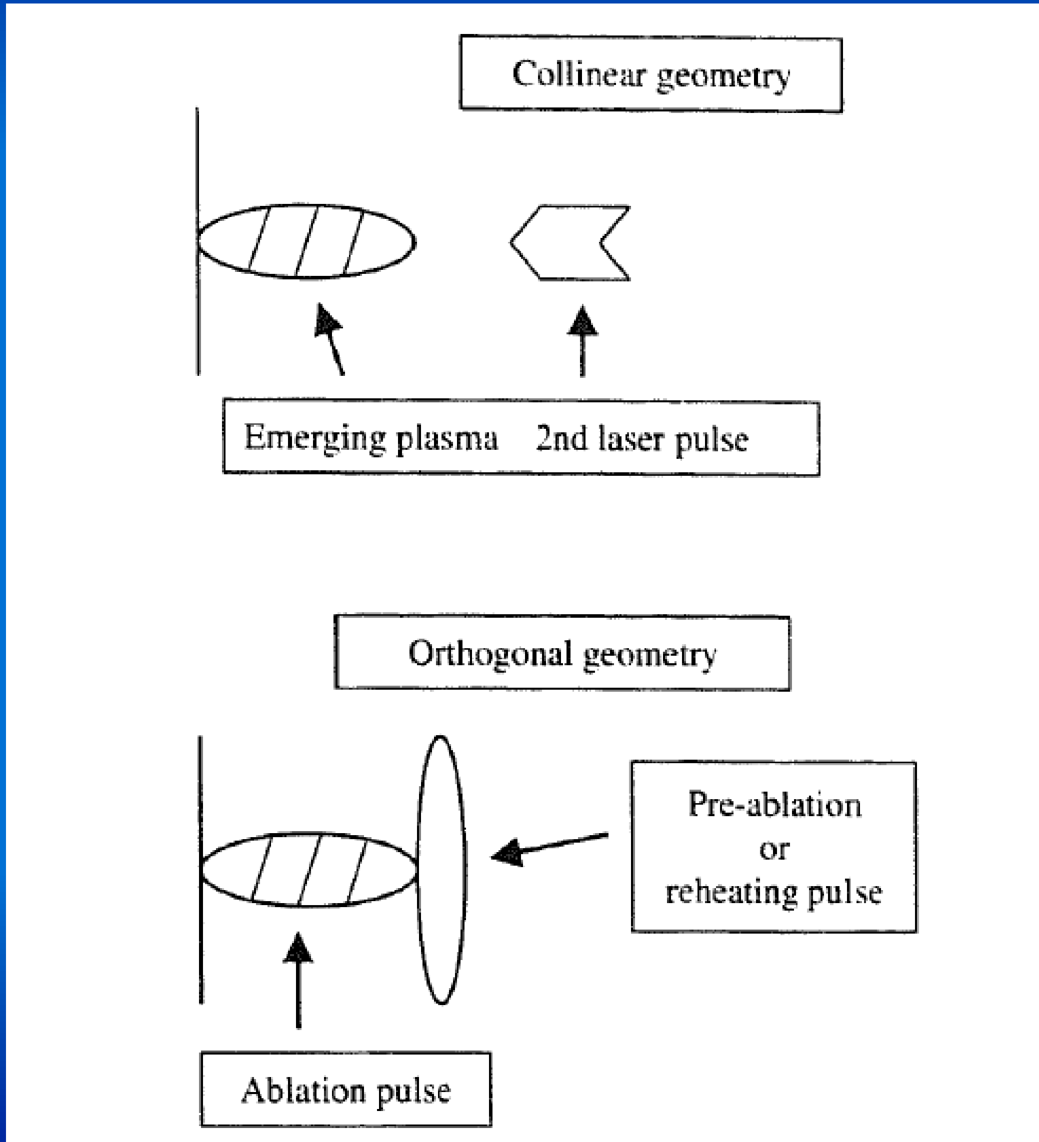

Double pulse technology -
collinear configuration

• single pulse – 80% energy is transformed in production of aerosol

• second pulse 90% of energy is absorbed in gas phase

– increasing of sensitivity (from 5 to 10x)

- decreasing of matrix effect

Duration between pulses from 0 to 20 us, dependent on laser configuration, element and sample type

– MHz repetition time!

NEXT generation – two color double pulse lasers

Double pulse technology - orthogonal configuration

- laser pulse is fired parallel to the sample surface
- before or after the perpendicular pulse hits the specimen

Laserová Ablace

- proces tvorby aerosolu
- uJ – mJ/cm2
- odpařování atomů a iontů z povrchu
- mnoho kritických parametrů
- energie, frekvence a vlnová délka

Laserová Ablace

Studies of laser wavelength on material removal from the sample surface have been performed by many researchers.[15,16] Dahmain[17] has also derived the mass-ablation rate with absorbed laser intensity I_a, laser wavelength λ, and atomic number Z based on experimental data for a laser energy lower than 10^{13} W cm^{-2} and $Z \leq 13$ (Equation 3):

$$m(\mathrm{kg\,s^{-1}\,cm^{-2}}) = 65\left(\frac{I_a\,\mathrm{W\,cm^{-2}}}{10^{13}}\right)^{5/9}\lambda^{-4/9}(\mu\mathrm{m})Z^{1/4} \quad (3)$$

Laserová Ablace

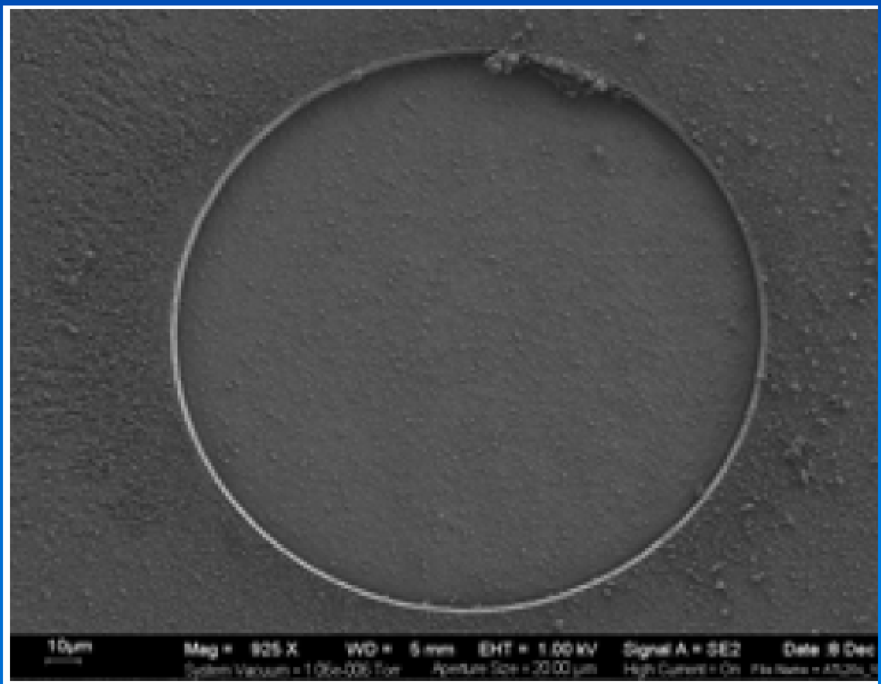

SEM of 100µm crater in glass

193 nm, 4 ns, 10 Hz, 100 shots, glass sample

Laserová Ablace

Figure 1: Image of 100um Quartz
Sample after 500 shots at 10 Hz

193 nm, 4 ns, 10 Hz, 500 shots, glass sample

Laserová Ablace

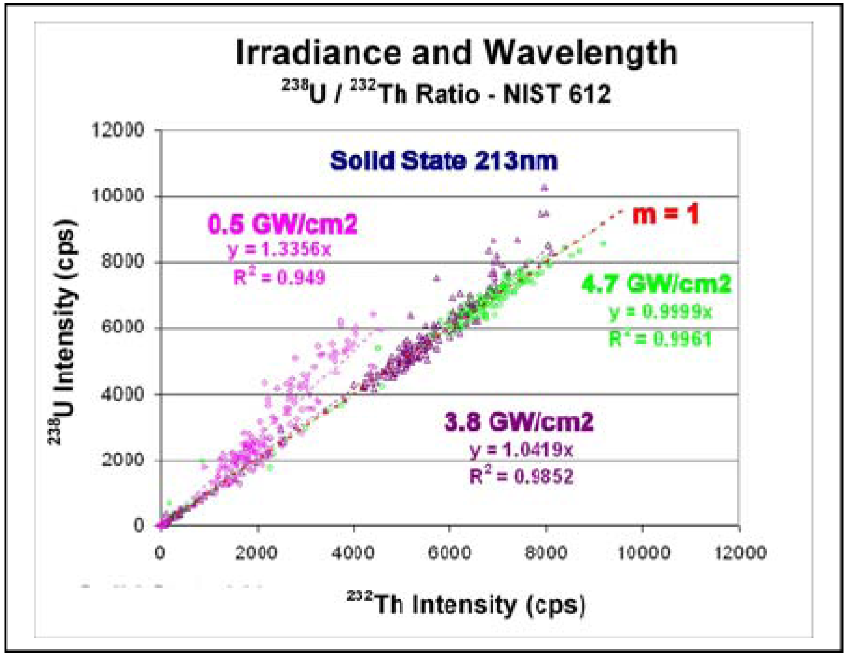

Figure 2: Irradiance and particle size effect on U/Th ratio (213nm)
With proper irradiance the longer 213nm wavelength is very effective in eliminating particle size induced fractionation.

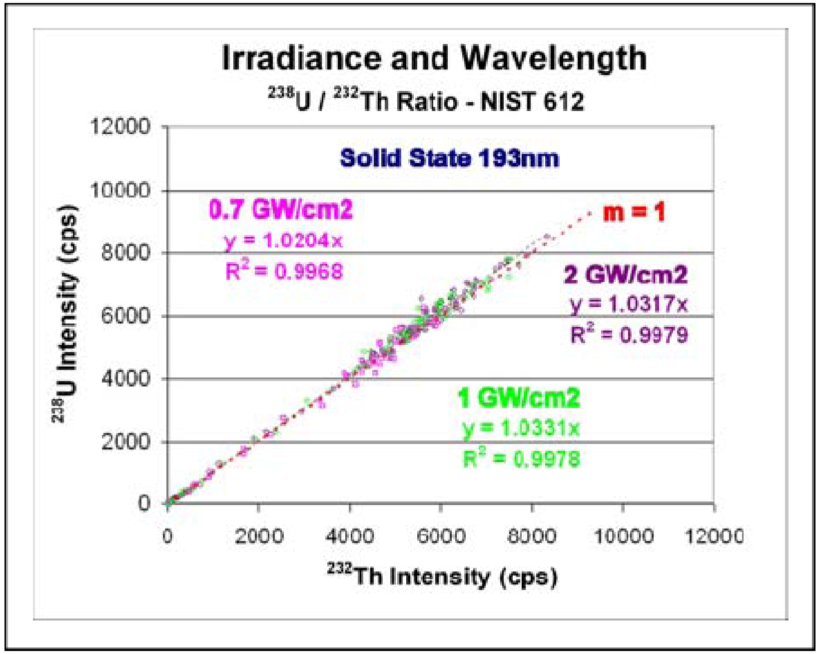

Figure 3: Irradiance and particle size effect on U/Th ratio (193nm)
A consistent U/Th ratio over a range of laser fluence benefits from the deep UV 193nm, short pulse width (sub 3 ns) of the UP-193 Solid State system.

Laserová Ablace

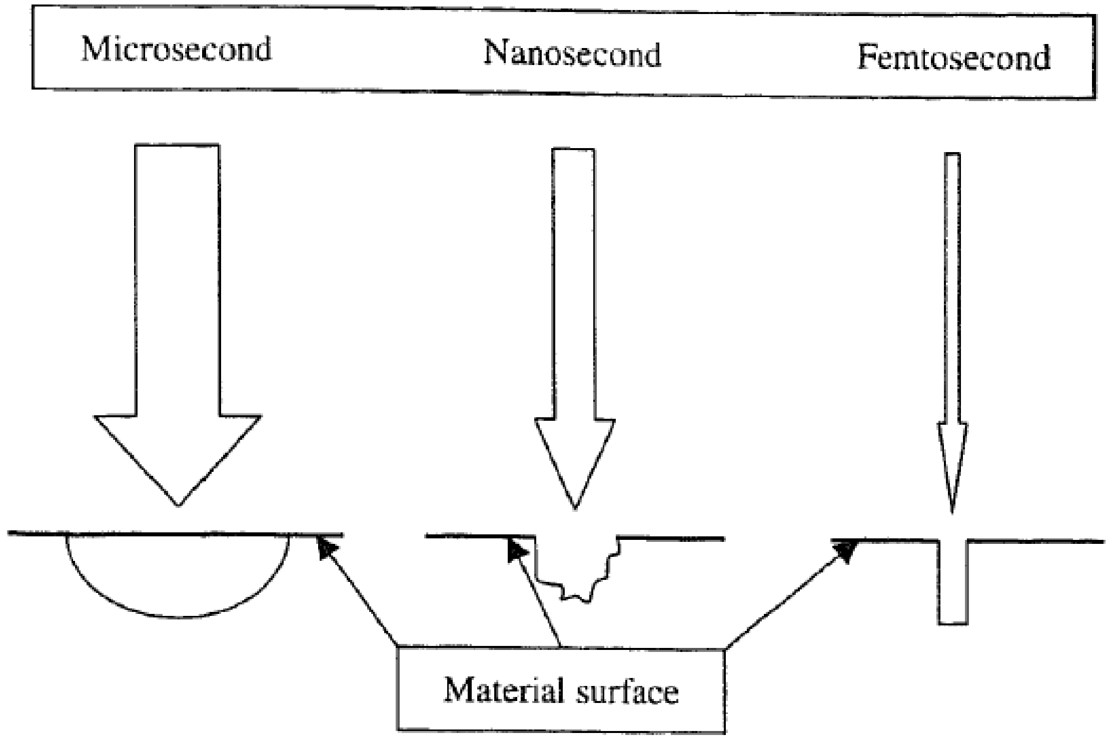

Figure 2.14 Schematics of the interactions of lasers with different pulse lengths on solid surfaces. The microsecond and nanosecond interactions proceed through heating, melting and vaporization. Pulses shorter than the plasma initiation time lead to direct vaporization and the ability, for example, to drill holes with precision